Geophysical Prospecting 31, 413–420, 1983.

MIGRATION BY EXTRAPOLATION OF TIME-DEPENDENT BOUNDARY VALUES*

G.A. McMECHAN**

ABSTRACT

McMECHAN, G.A. 1983, Migration by Extrapolation of Time-Dependent Boundary Values, Geophysical Prospecting 31, 413–420.

Migration of an observed zero-offset wavefield can be performed as the solution of a boundary value problem in which the data are extrapolated backward in time. This concept is implemented through a finite-difference solution of the two-dimensional acoustic wave equation. All depths are imaged simultaneously at time 0 (the imaging condition), and all dips (right up to vertical) are correctly migrated. Numerical examples illustrate this technique in both constant and variable velocity media.

INTRODUCTION

There are several schemes available for depth migration of zero-offset (or normal-moveout-corrected stacked) seismic sections. Among the common ones are Kirchhoff migration (French 1974, 1975), *f–k* migration (Stolt 1978), spatial deconvolution (Berkhout and Van Wulfften Palthe 1979, Berkhout 1980), and finite-difference methods (see Claerbout and Doherty 1972, Claerbout 1976). All involve some form of extrapolation based on the wave equation.

This paper describes a new finite-difference approach to migration that, for reasons that will become apparent, shall be referred to as *boundary value migration* (BVM). BVM is based on the reversibility of the wave equation; migration of a zero-offset section can be treated as the reverse of data modeling by the exploding reflector method. In this method, upward propagation of energy is initiated at all reflectors at time $t = 0$, the wave equation carries this energy through the model, and each recorder produces a response time history for all subsequent times.

The inverse problem of imaging reflectivity (i.e., migration) can be solved as a boundary value problem. The required boundary conditions over the recording surface are known at all times, and consist explicitly of the recorded observations.

* Received September 1981, revisions October 1982.

** Pacific Geoscience Center, Earth Physics Branch, Department of Energy, Mines and Resources, Sidney, BC V8L 4B2, Canada. Present address: Department of Computer Science, University of Victoria, PO Box 1700, Victoria, BC V8W 2Y2, Canada.

Migration is performed by driving the mesh at each recording point with the time reverse of the seismic trace recorded at that point. The wave equation propagates the energy downward into the medium; this extrapolation is continued backwards in time to $t = 0$, when all depths are imaged simultaneously.

The method is implemented with a two-dimensional, second-order-explicit, finite-difference solution of the two-way acoustic wave equation. Since no paraxial approximations are involved, even 90° dips are correctly migrated.

THEORY

In this section, the concept of migration as extrapolation of a data wavefield backwards in time (rather than the usual downward continuation in depth) is illustrated in the simple context of a point scatterer in a homogeneous half-space. In the following section, examples involving more complicated reflectors and heterogeneous velocity fields are presented.

The details of the formulation used for BVM by time extrapolation have been presented by McMechan (1982) in the context of imaging of earthquake sources. The examples in that paper are relevant here since migration also can be thought of as a source location problem in which sources are coincident with reflectors. Since the algorithm has been described by McMechan (1982), only a brief summary will be given here.

For use in illustrating the BVM technique, several synthetic zero-offset seismic data sections were generated by the exploding reflector method as referred to above. The finite-difference code used for this modeling is similar to that used for subsequent migration. The source function used in modeling was that presented by Alterman and Karal (1968). The absorbing boundary conditions described by Clayton and Engquist (1977) were used along the sides and bottom of the grid for both modeling and migration.

Energy is propagated through the finite-difference grid by the two-dimensional acoustic wave equation (see Claerbout 1976, Mitchell 1969):

$$U_{yy} + U_{zz} = \frac{1}{V^2(y, z)} U_{tt}, \tag{1}$$

where U is acoustic pressure, V is velocity, and subscripts denote partial derivatives with respect to y (the horizontal coordinate), z (the depth coordinate), or t (time). The model velocities V used in both modeling and migration are half the true velocities because total two-way traveltimes are twice the corresponding one-way times from the reflectors to the receivers. The acoustic wave equation is implemented in a second-order-explicit, finite-difference scheme. The characteristics of such schemes with respect to grid dispersion and numerical stability are discussed, among others, by Alford, Kelly and Boore (1974) and Mitchell (1969).

At a representative time step (at time t_i), three U wavefields are involved: $U(y, z, t_i)$ is the entire (y, z) wavefield at time t_i; $U(y, z, t_{i-1})$ is U at the previous time step $(t = t_{i-1})$; and $U(y, z, t_{i-2})$ is at t_{i-2}. The response $U(y_k, z_j, t_i)$ at the internal grid point (y_k, z_j) (located at the intersection of the jth horizontal mesh line with the kth vertical line) at time t_i is

$$\begin{aligned} U(y_k, z_j, t_i) = {} & 2(1 - 2A^2)U(y_k, z_j, t_{i-1}) - U(y_k, z_j, t_{i-2}) \\ & + A[U(y_{k+1}, z_j, t_{i-1}) + U(y_{k-1}, z_j, t_{i-1}) \\ & + U(y_k, z_{j+1}, t_{i-1}) + U(y_k, z_{j-1}, t_{i-1})], \end{aligned} \tag{2}$$

where $A = V(y_k, z_j)\,\Delta t/h$, Δt is the time step between successive U-wavefields ($\Delta t = t_i - t_{i-1}$), and h is the distance between grid lines in both y- and z-directions. The condition for local stability of (2) is that $\Delta t < hV^{-1}2^{-1/2}$.

The BVM processing of the synthetic zero-offset section corresponding to a point reflector in a homogeneous half-space is shown in fig. 1. Figure 1(a) contains the data section to be migrated. The finite-difference grid over which the wave equation is to be solved is defined in the y–z plane (a vertical slice through the earth). The process of migration transfers data from the y–t plane to the y–z plane as follows. Each iteration (each time step) during migration consists of two operations: the wave equation carries all the previous energy away from the upper boundary of the y–z plane (toward its migrated position); then, values extracted from the seismogram profile along that slice of constant time that corresponds to the current iteration are inserted at each recording point as new boundary conditions. These operations are facilitated by having the horizontal mesh increment equal to the data trace separation, and the time digitization increment of the data equal to the time step in extrapolation. [Interpolation (see Larner, Gibson and Rothman 1981) may be required.] Consider a specific example: fig. 1(b) shows the y–z plane at time t_i. All contributions for times greater than t_i are already present and are migrating toward their final positions. The boundary values to be inserted at time t_i are found in the seismogram profile (fig. 1a) along the slice at time t_i. Extrapolation continues backward in time with new boundary values inserted at each time step. The imaging condition is time 0. At this time, all the energy is at its migrated position; the entire y–z plane is imaged simultaneously (fig. 1d). This is in contrast to schemes such as that of Claerbout (1976), in which the data are downward-continued in depth (rather than time) to image one depth slice at each (depth) iteration.

In summary, solution of the forward problem involves generating a response wavefield $U(y, z, t)$ from initial conditions $U(y, z, t_1)$ and $U(y, z, t_2)$ in a velocity model $V(y, z)$. The resulting seismograms at $z = 0$ are $U(y, 0, t)$. In a real survey situation, $U(y, 0, t)$ are the recorded data. (For simplicity, $z = 0$ is indicated as the recording datum, but any (y, z) points can be used). Migration of the data consists of successively solving (2) with the boundary values $U(y, 0, t_i)$, $U(y, 0, t_{i-1})$, and $U(y, 0, t_{i-2})$ obtained directly from the observations at each i.

Although the point reflector example in fig. 1 is a simple one, it contains all the elements necessary for the construction of more complicated examples (and, in fact, for migration of real data, although application will be left for another paper). Any number of arbitrarily shaped reflections can be treated as the superposition of the responses to point sources (Huygens' principle), and the spatial variation of velocity $[V(y, z)]$ is already part of the finite-difference solution (see the equation above).

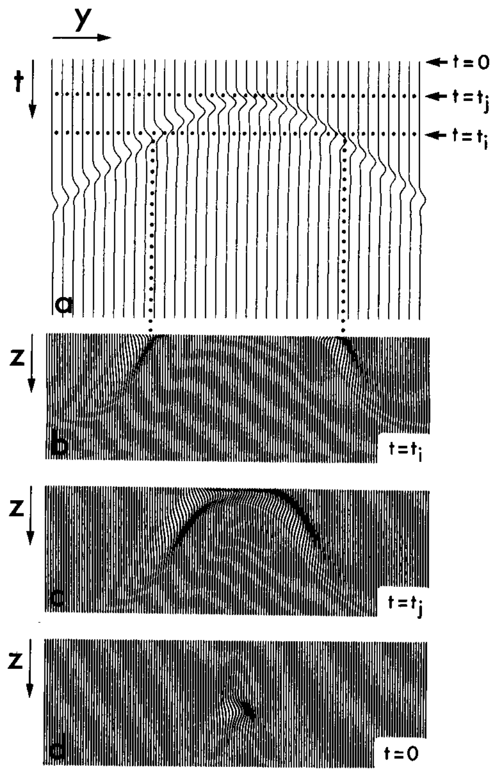

Fig. 1. Migration of data from a point reflector model. Panel (a) shows the synthetic zero-offset section computed for a point reflector model. Panels (b), (c), and (d) show the y–z plane (a vertical slice through the earth) at three iterations that are widely spaced in time. Time t_i is far from the image time, time t_j is intermediate, and $t = 0$ is the image condition. In (d), all the energy in the time section (a) has been successfully migrated back to the point reflector. The two small artifacts that remain faintly visible below the focus are due to the data truncation at the two edges of the profile. The dotted lines show the relationship between the seismograms and the boundary values in the y–z plane at $t = t_i$ (see text). For clarity, only every fourth seismogram that was computed is plotted in (a). In the migration, however, all the seismograms were used. This is also true of figs. 2, 3, and 4. Physical units are not included on the axes to emphasize that the method is independent of scale (e.g., very large-scale features can be imaged using long periods).

The following section contains three additional numerical examples of migration with the BVM method. In these examples, only the y–t plane and the imaged y–z plane will be shown; intermediate y–z plots such as fig. 1(b), (c) will not be included.

Numerical Examples

In the previous section, the method of boundary value migration was presented through an example of a point reflector. This section contains three additional

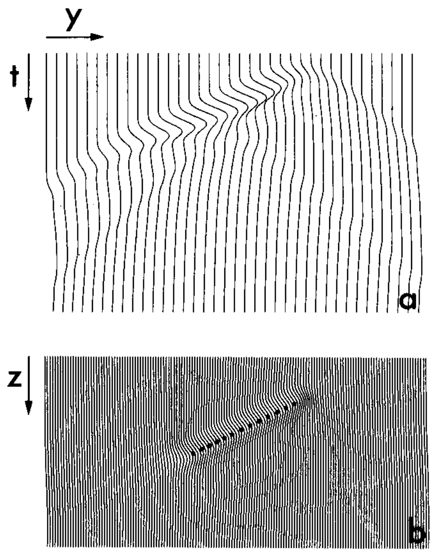

Fig. 2. Migration of a synthetic time section corresponding to a truncated, sloping reflector. Successive constant-time slices of the data section (a) are progressively introduced as boundary conditions and extrapolated backward in time with the two-way wave equation. The peak of the migrated reflector image in the y–z plane (b) coincides with the correct solution, which is shown as the dotted line. (See caption to fig. 1.)

examples that are representative illustrations of the technique. The examples are a truncated sloping reflector, a vertical reflector, and a sinusoidal reflector. In the first two, velocity is constant; in the third, it is a function of both y and z. Discussion of a broader range of applications is included.

Figure 2(a) contains the synthetic two-way time section for a truncated, sloping reflector. The diffractions generated at each end of the reflector are clear. Migration of this time section produces an image in the y–z plane as shown in fig. 2(b); the correct solution, which is a finite reflector dipping at 26.6°, is indicated by the dotted line.

Since the two-way wave equation is used in this migration algorithm, stable migration of very steep dips is possible. This is in contrast to other finite-difference algorithms that use an approximate (e.g. paraxial) one-way wave equation (see Claerbout 1976). The maximum dips that are correctly migrated by a paraxial approximation depend on the number of terms taken in the series expansion for the z extrapolation operator. Figure 3 illustrates migration of a vertical reflector (90° dip). Figure 3(a) contains the time section, and fig. 3(b) contains the migrated image. The dotted line in fig. 3(b) indicates the correct solution. Artifacts associated with spatial truncation of the data set, particularly at the right side, produce some broadening of the image.

Another potential advantage to the use of the two-way wave equation is that it can correctly migrate not only energy that moves monotonically downward in the

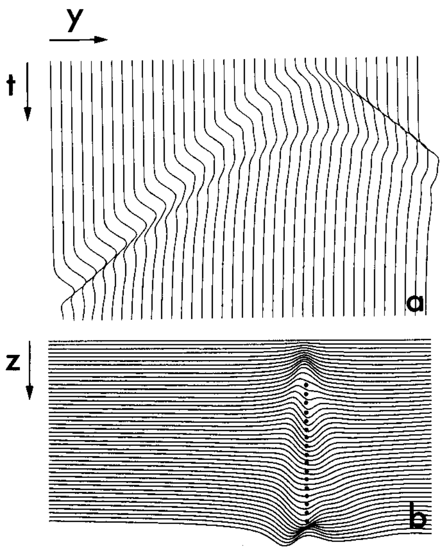

Fig. 3. Migration of a synthetic time section (a) corresponding to a vertical reflector. The peak of the migrated image in the y–z plane (b) coincides with the correct solution, which is shown as the dotted line. (See caption to fig. 1.)

z-direction during migration, but also energy whose migration path contains changes in the sign of $\partial z/\partial t$ (e.g., energy that leaves an exploding reflector downward). For example, it is possible to image the underside of an overhanging structure such as often occurs at the edge of a salt dome. For this energy to be recorded, it is necessary that there exists some deeper structure (such as a strong reflector, or a region of high velocity gradient) that turns the energy back toward the surface. Similarly, for this energy to be migrated properly, this deeper structure must be explicitly contained in the velocity field through which the migration is to be done. McMechan (1982) contains three examples of imaging of sources (for which one can directly substitute exploding reflectors) that use both up- and downgoing energy. It is of interest to note that this extension still conforms to the definition of Claerbout (1976) that a reflector exists at the spatial and temporal coincidence of up- and downgoing waves.

The final example of this paper, a sinusoidal reflector, is shown in fig. 4. This is a more complicated example than the previous ones, both in the shape of the reflector and in the velocity distribution. A linear velocity gradient was used in both y- and z-directions, with the velocity increasing from the upper left corner of the y–z grid to the lower right corner. The seismic time section (fig. 4a) was migrated to produce the sinusoidal image in the y–z plane (fig. 4b).

In all the examples shown above, migration by extrapolation of time-dependent boundary values has produced the correct solution. This migration technique, when applied to primary acoustic reflected waves, does not seem to have any problems or

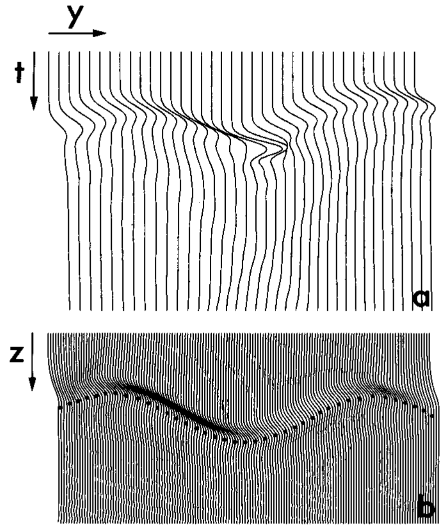

Fig. 4. Migration of a synthetic time section (a) corresponding to a sinusoidal reflector in a variable velocity medium. The peak of the migrated image in the y–z plane (b) coincides with the correct solution, which is shown as the dotted line. (See caption to fig. 1.)

inherent restrictions, other than those already associated with finite differences (see Alford et al. 1974), and these can generally be overcome by the use of a higher order difference scheme (only second order was used here), or by using higher data sampling rates or a finer computational mesh. The algorithm can also be used as it is for prestack migration by extrapolating data from each shot separately and then superimposing all the resultant y–z wavefields. The BVM algorithm should be directly applicable to real data in its present form; application is left for another paper. Finally, the concept of BVM is directly applicable in three, as well as two, space dimensions, requiring only a three-dimensional wave equation code for implementation.

Summary

A new method of migrating seismic time sections in variable velocity media is presented and illustrated with four numerical examples. The data are introduced in successive time slices as boundary conditions to a finite-difference extrapolation backwards in time. At time 0 (the imaging condition), all depths are imaged simultaneously. Extrapolation through time is done with the two-way wave equation so all dips are correctly migrated. The method is easy to implement and has no inherent limitations other than those typically associated with finite differencing.

Acknowledgments

The author gratefully acknowledges critical reviews by his colleagues in the Earth Physics Branch and by C. Yorath of the Geological Survey of Canada. Primary funding of this project was by the Department of Energy, Mines & Resources, Canada; additional support was provided by I. Barrodale through NSERC grant A5251. All computations were performed at the Computing Center of the University of Victoria. Contribution from the Earth Physics Branch No. 1025.

References

ALFORD, R.M., KELLY, K.R. and BOORE, D.M. 1974, Accuracy of finite-difference modeling of the acoustic wave equation, Geophysics 39, 834–842.

ALTERMAN, Z. and KARAL, F.C. 1968, Propagation of elastic waves in layered media by finite difference methods, Bulletin of the Seismological Society of America 58, 367–398.

BERKHOUT, A.J. 1980, Seismic Migration, Elsevier, New York.

BERKHOUT, A.J. and VAN WULFFTEN PALTHE, D.W. 1979, Migration in terms of spatial deconvolution, Geophysical Prospecting 27, 261–291.

CLAERBOUT, J.F. 1976, Fundamentals of Geophysical Data Processing, McGraw-Hill, New York.

CLAERBOUT, J.F. and DOHERTY, S.M. 1972, Downward continuation of moveout corrected seismograms, Geophysics 37, 741–768.

CLAYTON, R.W. and ENGQUIST, B. 1977, Absorbing boundary conditions for acoustic and elastic wave equations, Bulletin of the Seismological Society of America 67, 1529–1540.

FRENCH, W.S. 1974, Two-dimensional and three-dimensional migration of model-experiment reflection profiles, Geophysics 39, 265–277.

FRENCH, W.S. 1975, Computer migration of oblique seismic reflection profiles, Geophysics 40, 961–980.

LARNER, K., GIBSON, B. and ROTHMAN, D. 1981, Trace interpolation and the design of seismic surveys (abstract), Geophysics 46, 407.

MCMECHAN, G.A. 1982, Determination of source parameters by wavefield extrapolation, Geophysical Journal of the Royal Astronomical Society 71, 613–628.

MITCHELL, A.R. 1969, Computational Methods in Partial Differential Equations, J. Wiley & Sons, New York.

STOLT, R.H. 1978, Migration by Fourier transform, Geophysics 43, 23–48.